Results in Materials 8 (2020) 100131

Contents lists available at ScienceDirect

Results in Materials

journal homepage: www.journals.elsevier.com/results-in-materials

Study of an exhumed HDPE geomembrane used in an industrial water pond: Physical and thermoanalytical characterisations

Fernando Luiz Lavoie [a,b,*], Marcelo Kobelnik [b], Clever Aparecido Valentin [b], Jefferson Lins da Silva [b], Maria de Lurdes Lopes [c]

[a] Mauá Institute of Technology, São Caetano Do Sul, SP, Brazil
[b] University of São Paulo - USP, São Carlos School of Engineering, EESC, São Carlos, SP, Brazil
[c] University of Porto, Department of Civil Engineering, Porto, Portugal

ARTICLE INFO

Keywords:
High-density polyethylene
TG
DSC
TMA
Physical tests

ABSTRACT

This paper analyzed the behavior of an HDPE geomembrane exhumed sample used for 2.25 years as a liner in an industrial water pond from a Brazilian company, as well as another similar sample as a reference. The thermogravimetry (TG) using different heating rates under synthetic air purge gas evaluation showed that the exhumed sample presented a different behavior in the TG curve for a heating rate of 5 °C min^{-1} attributed to the reaction time. The thermomechanical analysis (TMA) curves without purge gas showed the range of thermal stability between 30 and 65 °C for the reference sample, which is attributed to a molecular relaxation. The exhumed sample does not have the same relaxation, probably because this sample was submitted to severe environmental conditions in the field. Finally, the physical property values for the exhumed sample showed mechanical brittle behavior, which can indicate that changes probably occurred in the polymer structure.

1. Introduction

A geomembrane can be defined as a polymeric sheet with very low permeability produced with smooth faces or textured ones in different colors used in environmental applications, such as landfills and treatment ponds, in transportation and geotechnical applications, especially in tailing dams. It can also be used in agriculture, such as water ponds, liquid waste ponds and irrigation canals [1–4].

Based on information from domestic manufacturer's, in Brazil about a hundred million square meters of HDPE geomembranes have been installed over 20 years, initially in landfills and mining facilities. However, over the last decade, they have been more widely used for water ponds and liquid waste ponds, aquaculture ponds and irrigation canals.

HDPE geomembranes have been studied using different evaluation parameters, such as ultraviolet radiation during exposure to sun [5–7], chemical environment [8,9], moisture [10], thermal and mechanical stresses [5], atmospheric pollution and microbiological activity [5]. These parameters can cause changes in the polymer structure, leading to degradation mechanisms. These mechanisms can induce molecular chain scission, crosslinking and bond breaking [5,6].

Mendes et al. [11] analyzed the thermal and mechanical properties of commercial high-density polyethylene without additives after weathering for 4440 h in the city of Rio de Janeiro. The test results showed a huge environmental oxidative degradation of the polymer, including the change in mechanical behavior from ductile to brittle in 2520 h and an increase in the crystallinity.

The polymer protection for HDPE geomembranes is normally ensured by adding carbon black (2–3%) and other additives, such as antioxidants and thermostabilizers in varying proportions (0.5–1.0%). Through the service life of the geomembrane, some degradation mechanism or aging over time will cause it to fail, in general by a synergic combination of physical and chemical aging [12,13].

Noval et al. [14] evaluated an exhumed HDPE geomembrane applied as a liner in the San Isidro pond, in the Canary Islands, Spain. Different analyses were performed to understand the behavior of this geomembrane. The authors evaluated the physical properties, mechanical properties, carbon black content, crystallinity, oxidative induction time and microscopy analysis of the samples from the south and north slopes. By scanning electron microscopy, the authors were able to find superficial cracks in the samples from the south and north slopes after 162 and 174 months of exposure. The mechanical behavior by tensile stress was followed over 20 years and a huge variation was observed over the years.

* Corresponding author. Mauá Institute of Technology, São Caetano Do Sul, SP, Brazil.
E-mail address: fernando.lavoie@maua.br (F.L. Lavoie).

https://doi.org/10.1016/j.rinma.2020.100131
Received in revised form 4 July 2020; Accepted 4 August 2020
Available online 22 August 2020

The elongation at break decreased less than 50% of the original value and reached the half-life of the product. Using the Arrhenius model, the authors estimated the time for antioxidant depletion for both samples. The time estimated is 58 years for the sample from the north slope and 47 years for the sample from the south slope.

It is not common to use thermoanalytical methods, such as Thermogravimetry (TG) and Thermomechanical Analysis (TMA) to evaluate behavior changes in exhumed or aged geomembranes. Mitchell [15] used the Differential Scanning Calorimetry (DSC) to study the crystallinity changes of an HDPE geomembrane immersed in synthetic leachate from a uranium mill. The crystallinity results were 52.3, 51.5, 53.4, and 55.7%, respectively for the virgin sample, immersed at 18, 47 and 76 °C. Dix and Burkinshaw [16] measured the heat required to melt some high-density polyethylene resins and their melting points by DSC analyses. According to the authors, there was a tendency towards lower melting points and heat fusion with a decrease in resin densities.

Lodi and Bueno [17] exposed two HDPE geomembranes with 0.8 and 2.5 mm of thickness to weathering for 30 months. They used the TG with purge gas of synthetic air with a heating rate of 20 °C min^{-1} to analyze the changes that occurred with the exposure. For the thinner sample, the temperature for the beginning of the mass loss was 420 °C, but the exposed sample presented 440 °C. According to the authors, the temperature for the beginning of the mass loss for HDPE is about 470 °C. The 2.5 mm thick exposed sample presented a very similar curve to the virgin sample.

Lavoie et al. [18] utilized mechanical tests and Thermogravimetry Analysis (TGA) to understand the polymer behavior of a 2.0 mm thick HDPE geomembrane immersed for 4 months in leachate from vinasse solution from sugarcane production. The results showed no changes in the thermal stability between the virgin sample and the exposed sample and the decrease in the mechanical properties of about 30%.

Abdelaal et al. [19] evaluated HDPE geomembranes exposed to high temperatures and studied the annealing effects for the polymers using DSC. The changes in the melting point between the virgin and aged samples were clear, especially for the samples with the highest temperature and longest times of incubation. The melting point tended to increase when the temperature incubation rose for long periods.

Valentin et al. [20] used TG, Differential Thermal Analysis (DTA), Differential Scanning Calorimetry (DSC) and Dynamical Mechanical Analysis (DMA) to evaluate different HDPE geomembranes from several manufacturers in Brazil, where the authors showed that there were different behaviors in thermoanalytical evaluations. DSC analysis showed that the second heating provided a narrower curve than the first heating. The DMA results showed a slight increase in the thinner sample analyzed and no changes for the other samples.

Thus, to help understand the HDPE geomembranes exposed due to water pond applications, this paper evaluated the thermoanalytical, physical and mechanical behavior of two HDPE geomembranes; one exposed and another a virgin sample as a reference.

2. Material and methods

2.1. Materials

The present study evaluated two HDPE geomembrane samples of 1.0 mm nominal thickness; one exhumed by an industrial water pond (called GM CLIQ) with 2.25 years of exposure and, the other sample, a virgin geomembrane (called GM 1L) having similar characteristics to the exhumed sample, used as a reference. Fig. 1 shows the industrial water pond geomembrane before the exhumation, in service. Fig. 2 shows the industrial water pond after recuperation with a new HDPE geomembrane. It was decided to recuperate it due to the lack of an adequate drainage system and the poor installation service, including the defects in the connection between the geomembrane and the concrete structures of the pond and the waves in the geomembrane panels. Unfortunately, in Brazil it is not common to save and store geomembrane samples to the

Fig. 1. The industrial water pond geomembrane before the exhumation, in service.

Fig. 2. The industrial water pond after being recuperated with a new HDPE geomembrane.

product installed in the field to monitor the properties of the material during the service life of the work. HDPE geomembranes are manufactured to provide a long-term life, around decades, even when exposed to the weather, guaranteeing the retention of product properties. In Brazil, some geomembranes have polyethylene resins with low stress cracking resistance, additive packages without HALS (hindered amine light stabilizers) and sometimes off-grade resins. Such types of products can have a short-term life, causing environmental and financial losses.

For this study, the samples were tested using thermoanalytical methods, such as TG, DSC, and TMA. Physical and mechanical tests were also conducted to compare exhumed and reference samples.

2.2. Physical properties

The thickness [21] was determined by measuring the difference between the dead-weight loading gauge and the geomembrane specimen thickness with 0.001 mm precision, applying a pressure force of 200 ± 0.2 kPa. Density measurement [22] was performed in isopropyl alcohol at 21 ± 0.1 °C, mass sample 1.0 g ± 0.1 g in apparatus that included an analytical balance with a 0.0001 g precision and an immersion vessel and a beaker. The flow rates (MFR) [23] of the studied samples were obtained

using a plastometer with a smooth bore 2.095 ± 0.005 mm in diameter and 8.000 ± 0.025 mm long. The polymer was extruded at 190 ± 0.08 °C with a dead-weight load of 5.0 kg and its mass was measured for 10 min using an analytical balance with a 0.0001 g precision.

2.3. Mechanical properties

Mechanical tests were performed using an EMIC Universal Machine, model DL 3000 with pneumatic grips and a 2-kN load cell. The tests were performed with test speeds of 50, 51 and 300 mm min^{-1}, respectively, for the tensile [24], tear [25] and puncture [26] tests.

2.4. Methodology used for thermoanalytical evaluation

The thermoanalytical evaluation was carried out by TG, Differential Scanning Calorimetry (DSC) and TMA. For the TG curves, samples were analyzed by a TA Instrument model SDT 2960 using synthetic air purge gases, carbonic air, both with a flow of 110 mL min^{-1}, in an alumina crucible using heating rates of 5, 10, 20, and 30 °C min^{-1}. The specimens were cut by a circular section mold of 3 mm^2. The Thermomechanical Analysis (TMA) was performed using a TA Instrument, SDT 2940 model. The samples were submitted to purge gases of synthetic air and nitrogen, with a flow of 50 mL min^{-1} and a heating rate of 5 °C min^{-1}. Additionally, the TMA analyses were performed in an environment oven without purge gas flows. The DSC curves were performed in Mettler Toledo equipment, DSC1 Stare model, with an alumina crucible, using nitrogen gas purge with a flow of 50 mL min^{-1} and heating rates of 10 and 30 °C min^{-1} for the glass transition study. Besides, the samples were heated and cooled in a temperature range of −80 to 200 °C. For the activation energy study, the four TG curves were utilized for kinetic evaluation, using the Flynn-Wall-Ozawa method, which does not need to use kinetic models [20,27].

3. Results and discussion

3.1. Thermoanalytical evaluations

Recently, Valentin et al. [20] studied four HDPE geomembrane samples with different thicknesses, virgin samples (new samples), widely marketed in Brazil. This study was conducted under synthetic air and nitrogen purge gases. The present work presents two different samples of HDPE geomembranes, with similar thicknesses. The evaluation of the exhumed sample is, therefore, valid for comparison purposes. It is important to mention that there are no regulations in terms of sampling of the product applied on site. Thus, the use of reference materials is limited to similar materials.

Figs. 3 and 4 show the TG and DTG curves under synthetic air for the exhumed and reference samples, respectively. It can be observed that the TG curves at 5–10 °C and 20–30 °C are similar. This behavior is not seen in the TG curves for the exhumed sample because the 5 °C analysis showed a different behavior to the others. For both samples, this behavior is attributed to the effect of the reaction time due to the different heating rates, highlighting the reference sample which showed that the reaction was only for the heating rate of 5 °C min^{-1}. Figs. 3B and 4B showed the DTG curves and the reactions occurring for different heating rates can be seen. The DTG behavior for the exhumed sample shows that when the heating rate is increased, the overlapping reactions tend to decrease gradually. For the reference sample, the thermal behavior showed the tendency to decrease the number of decomposition reactions. The reference sample evaluated in this paper has a synthetic air thermal decomposition similar to that observed in the study by Valentin et al. [20]. Besides that, the TG/DTG-DTA curves were performed in triplicate to verify the repeatability of the obtained curves. Table 1 shows the values of the mass variation obtained under synthetic air for both samples.

The TG/DTG curves for the thermal decomposition study for the exhumed sample and reference sample under carbonic gas are shown in Fig. 5A and B, respectively. In both samples, there was thermal behavior which presented a shoulder at the beginning of the thermal decomposition for the heating rate of 5 °C, and additionally for the heating rate of 10 °C for the reference sample. As an exception to these reactions, the other heating rates presented a one-stage of heating, without a change in the DTG curves, which indicates a homogeneous kinetic behavior of the decomposition thermal reaction. Table 2 shows the mass variation values for each heating rate studied.

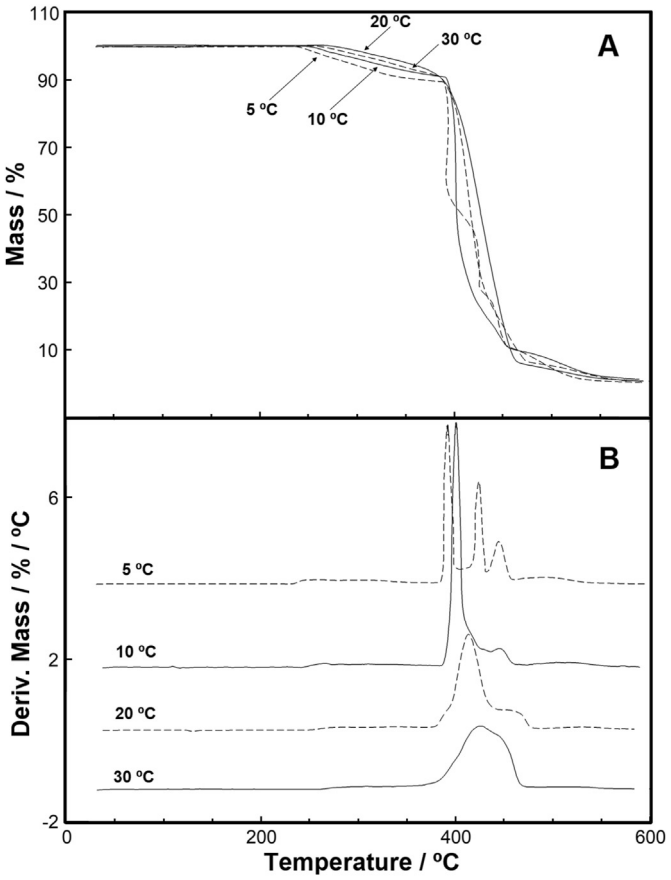

Fig. 3. (A) TG curves under synthetic air purge gas, with a mass sample of about 3.50 mg for the exhumed sample and (B) DTG curves of TG curves, under synthetic air purge gas for the exhumed sample.

The kinetic analysis is shown in Fig. 6 and was obtained from the DTG curves of the reference and exhumed samples, as seen in Figs. 3–5. The activation energy values for the sample in synthetic air were obtained for the first stage of thermal decomposition for the two samples. The activation energy *versus* conversion degree, for the analyses carried out in synthetic air, showed that for both samples the values are very similar and have lower values than those obtained in carbonic gas. This fact is attributed to the polymer oxidation reaction with synthetic air, which causes the activation energy to decrease and does not occur in carbonic gas, where the reaction occurs only due to the decomposition of the polymer itself. In a study on bicuiba oil, Kobelnik et al. showed that the activation energy values in oxygen gas are higher than those obtained in nitrogen [28]. For both samples, in carbonic gas, the kinetic behaviors are different from each other at the beginning of the thermal decomposition but very similar to the degree of conversion 0.3. The mean values of the activation energy are shown in Table 3, where the values of the correlation coefficient adjustments are also presented and indicate a good linear relationship of the obtained kinetic data.

Additionally, Fig. 7A and B show the DTA curves respectively for the exhumed and reference samples for different heating rates. For both

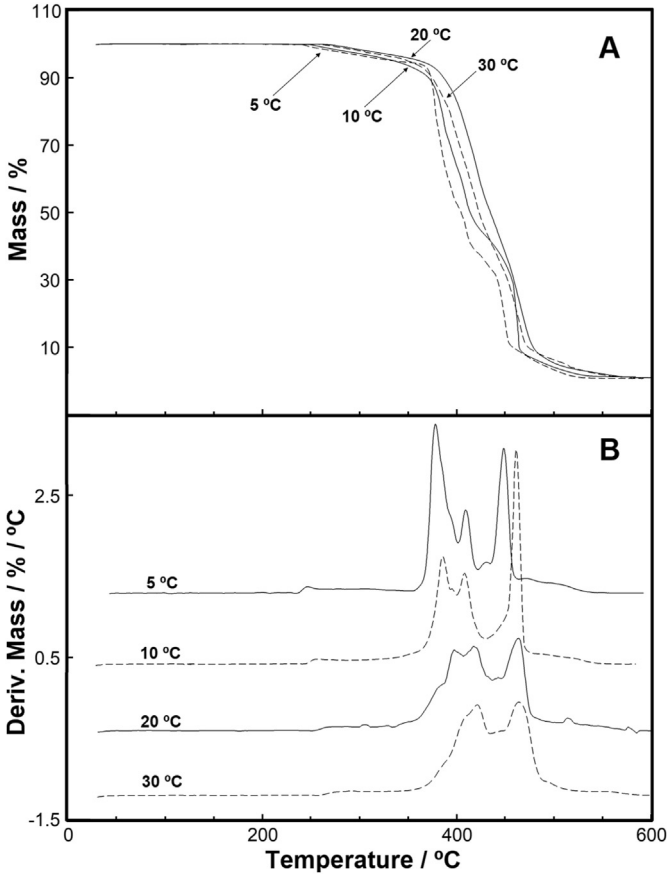

Fig. 4. (A) TG curves under synthetic air purge gas, with a mass sample of about 3.50 mg for the reference sample and (B) DTG curves of TG curves, under synthetic air purge gas for the reference sample.

samples, the endothermic peak can be seen between 120 and 140 °C due to the material melting, and according to the behavior seen in the DSC curves. The first stage of thermal decomposition shows that there is an exothermic event between 230 and 290 °C, while from the second stage of decomposition, there are different DTA curve behaviors. As can be seen in the exhumed sample at 5 °C, from the second stage of mass loss there is a combustion behavior of the sample, which caused the DTA curve to distort in the first peak and rise in the second peak. The third peak shows that the last stage is a decomposition final material exothermic reaction. For the exhumed sample, the peaks showed no combustion, which was attributed to exothermic reactions of the sample. Besides that, for the reference sample, the fact that a reaction could not be seen can be attributed to the combustion for different heating rates. In this sample, the presence of different exothermic peaks can be observed during the thermal decomposition.

Figs. 8 and 9 show the DSC curves of heating and cooling, respectively, in the temperature range from −80 to 200 °C in two heating rates. The aim of using two heating rates was to verify the glass transition. Fig. 8 shows, for the 10 °C min^{-1} analysis, that there was a change between −70 and −60 °C at the baseline, which was attributed to the glass transition in both samples. This change in the baseline can be seen for the analysis of 30 °C min^{-1}, but in the temperature range from −56 to 24 °C. For the melting point, it can be observed for the analysis of 10 °C min^{-1} that the exhumed sample has an overlapping reaction while the reference sample does not have an overlapping reaction for the analysis of 30 °C min^{-1}. It can be observed that there was no overlapping reaction for the exhumed sample. In addition, there was an increase in melting peaks, which is usually explained by high heating rates. Fig. 9 shows that the crystallization behavior for both samples is coincident and can be seen

Table 1
Temperature range obtained by DTG curves for the thermal decomposition stages under synthetic air purge gas, with heating rates of 5, 10, 20 and 30 °C min^{-1}.

Compound/purge gas	Stage	Heating rate/ °C	ΔT/°C	Mass loss/ %
Reference sample (synthetic air)	1	5 °C	233–254	5.53
	2		254–401	42.11
	3		401–434	19.00
	4		434–463	24.44
	5		463–550	8.30
	Residue		550	0.62
Exhumed sample (synthetic air)	1	5 °C	232–383	10.67
	2		383–405	38.52
	3		405–432	25.02
	4		432–460	15.71
	5		460–475	10.08
	Residue		475	0.00
Reference sample (synthetic air)	1	10 °C	243–356	7.12
	2		356–428	49.10
	3		428–475	36.60
	4		475–550	5.83
	Residue		550	1.35
Exhumed sample (synthetic air)	1	10 °C	236–385	9.00
	2		385–435	72.37
	3		435–463	8.76
	4		463–585	8.63
	Residue		585	1.24
Reference sample (synthetic air)	1	20 °C	251–345	4.52
	2		345–443	59.15
	3		443–484	28.13
	4		484–590	7.17
	Residue		590	1.03
Exhumed sample (synthetic air)	1	20 °C	244–375	8.35
	2		375–446	73.03
	3		446–481	12.75
	4		481–575	5.23
	Residue		575	0.65
Reference sample (synthetic air)	1	30 °C	257–340	3.55
	2		340–434	46.16
	3		434–535	47.46
	4		535–590	1.82
	Residue		590	1.01
Exhumed sample (synthetic air)	1	30 °C	256–364	6.47
	2		364–476	88.47
	3		476–590	4.67
	Residue		590	0.39

for both samples.

Fig. 10 shows the TMA curves obtained under synthetic air purge gas and without purge gas. It is important to highlight that each sample was set in the equipment oven for 10 min before starting the analyses in order to homogenize the thermal behavior. Moreover, it can be observed that both samples, without purge gas, have thermal stability until a temperature of about 30 °C. From this temperature, it can be seen that both samples have a thickness decrease until 110 °C. It was observed that the reference sample has a range between 30 and 65 °C, which is attributed to a molecular relaxation. The same effect was not observed for the exhumed sample because it was subjected to severe environmental conditions, and therefore due to continuous exposure of the sample, relaxation no longer occurred.

Both samples present a distinct behavior without a purge gas condition. As can be seen in the dynamic purge gas, in this condition both samples show no change in thickness, which was attributed to the cooling effect of the sample during heating. Due to the possibility of reaction between the sample and the synthetic air purge gas, the analysis was repeated under nitrogen purge gas and the result was strictly the same, indicating the behavior of the samples.

3.2. Physical evaluations

Tables 4 and 5 show the results from the physical properties for both analyzed samples. The Geosynthetic Research Institute GM-13 [29] is a

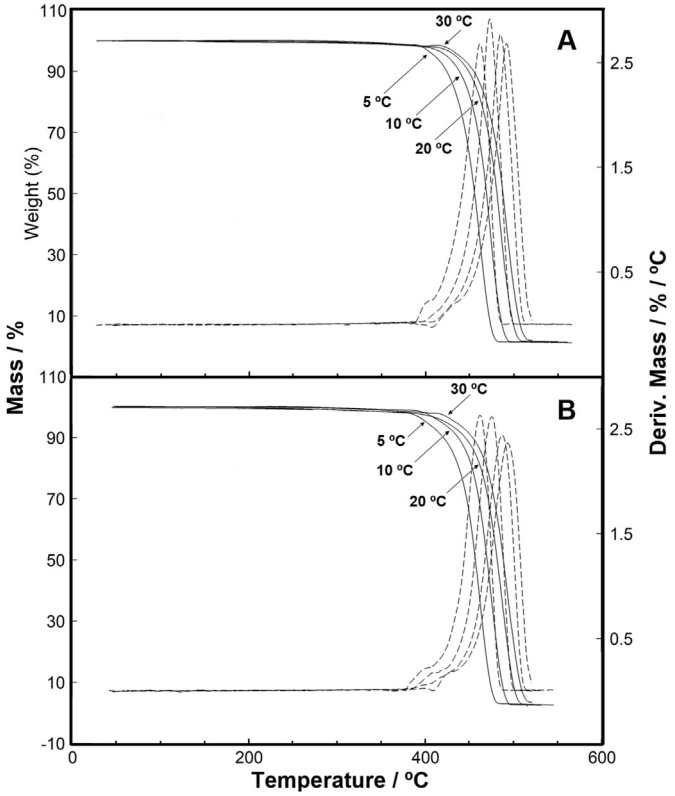

Fig. 5. TG/DTG exhumed sample curve (A) and reference sample curve (B), under carbonic gas purge gas with a flow through to 110 mL min^{-1}, with mass samples of about 3.50 mg using different heating rates, in an alumina crucible.

Table 2
Temperature range obtained by DTG curves for the thermal decomposition stages under carbonic gas purge gas, with heating rates of 5, 10, 20 and 30 °C min^{-1}.

Compound/purge gas	Stage	Heating rate/ °C	ΔT/°C	Mass loss/ %
Reference sample (carbonic gas)	1	5 °C	376–490	95.75
	Residue		490	4.25
Exhumed sample (carbonic gas)	2	5 °C	389–489	97.17
	Residue		489	2.83
Reference sample (carbonic gas)	1	10 °C	382–498	96,01
	Residue		498	3.99
Exhumed sample (carbonic gas)	4	10 °C	397–507	96.78
	Residue		507	3.22
Reference sample (carbonic gas)	4	20 °C	391–518	95.68
	Residue		518	4.32
Exhumed sample (carbonic gas)	4	20 °C	408–516	96.36
	Residue		516	3.64
Reference sample (carbonic gas)	3	30 °C	409–530	94.92
	Residue		530	5.08
Exhumed sample (carbonic gas)	1	30 °C	412–522	96.59
	Residue		522	3.41

standard specification intended to normalize the virgin HDPE geomembranes for manufacturing quality control. Exhumed geomembranes with property values lower than this standard specification minimum values can help us to understand changes in the polymer morphology. The nominal thickness of both samples is 1.0 mm, and the values obtained were close to the nominal value. The density values showed that the reference sample has a higher density than the exhumed sample. Both samples are in accordance with the Geosynthetic Research Institute criteria. The melt flow rate results showed low values for both tested samples and it was observed which exhumed sample had a higher viscosity than the reference sample. The tensile test values of the samples showed a better behavior for the reference sample than the exhumed

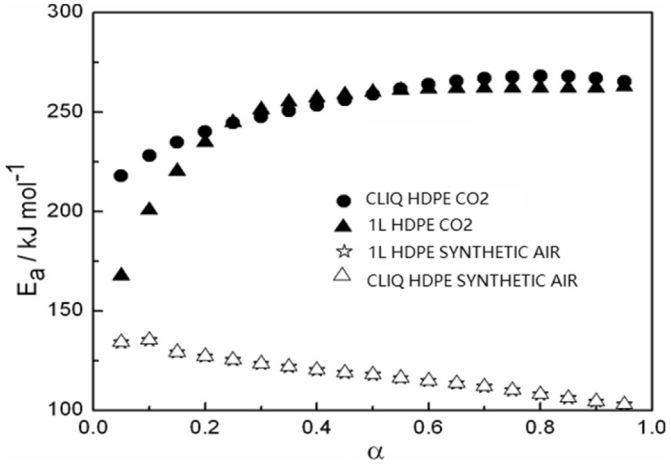

Fig. 6. Kinetic evaluation from exhumed and reference samples under carbonic gas and synthetic purge gases.

Table 3
$Ea/kJ\ mol^{-1}$ and correlation coefficient (r) for the thermal decomposition stages.

Compound	Sample mass	$*E_a/kJ\ mol^{-1}$	$*r$
CLIQ	(carbonic gas) 1st decomposition stage	254.01 ± 0.06	0.99028
	(synthetic air) 1st decomposition stage	118.00 ± 0.08	0.99498
1L	(carbonic gas) 1st decomposition stage	247.71 ± 0.10	0.98667
	(synthetic air) 1st decomposition stage	121.64 ± 0.09	0.99497

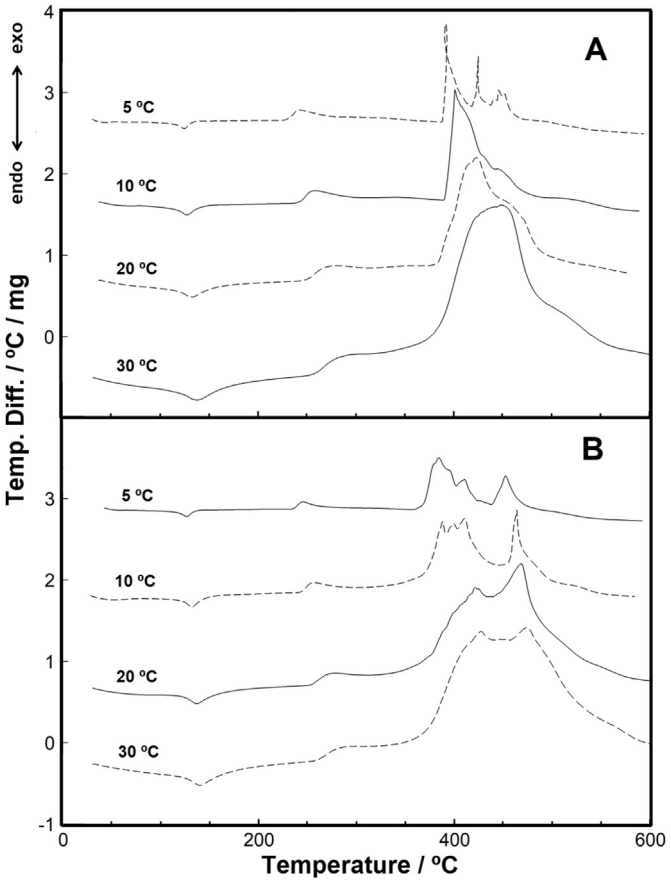

Fig. 7. DTA curves of the samples for different heating rates. (A) Exhumed sample and (B) reference sample.

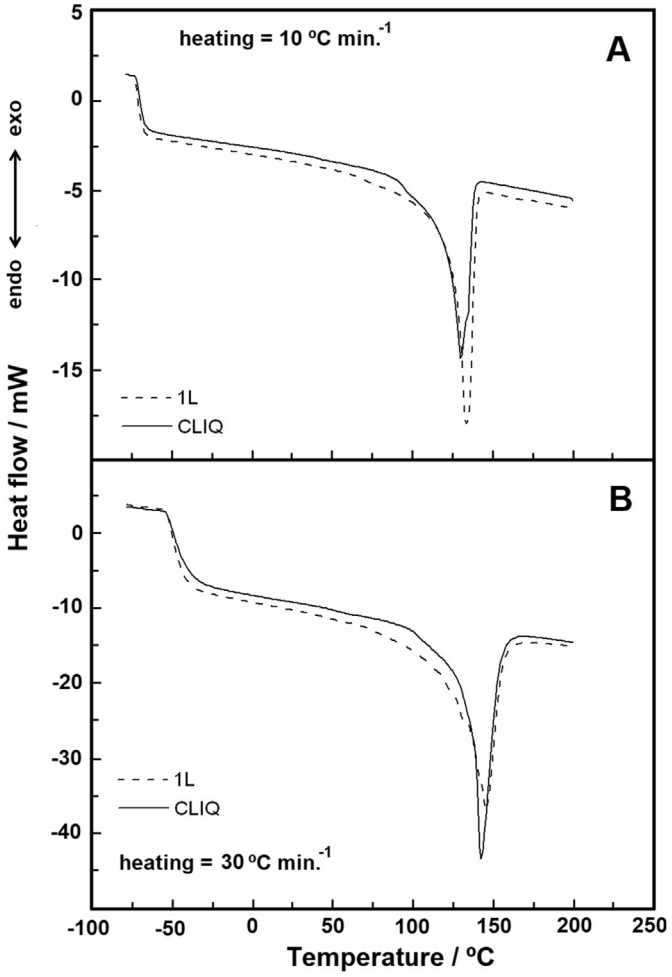

Fig. 8. DSC curves showing the samples' melting point for heating rates of 10 and 30 °C min^{-1} under nitrogen purge gas with a flow through to 50 mL min^{-1}, with mass samples of about 3.50 mg in an alumina crucible.

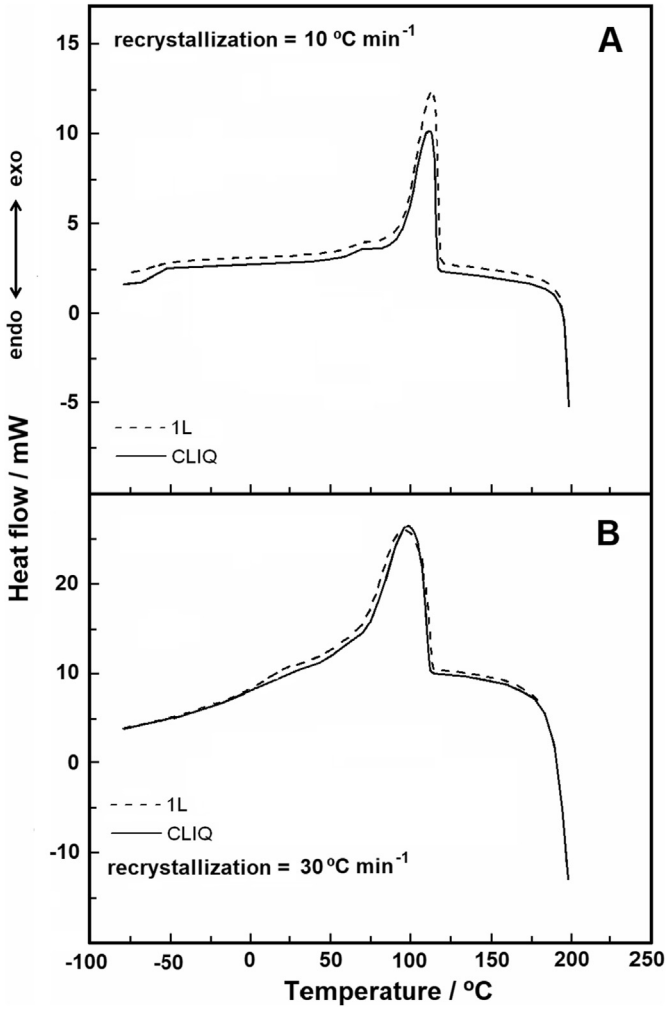

Fig. 9. Crystallization DSC curves for heating rates of 10 and 30 °C min^{-1} under nitrogen purge gas with a flow through to 50 mL min^{-1}, with mass samples of about 3.50 mg in an alumina crucible.

sample, especially for the tensile break resistance and elongation. These were not in accordance with the Geosynthetic Research Institute criteria for the exhumed sample. Figs. 11 and 12 show the tensile test curves for the exhumed and reference samples, respectively. The reference sample shows a typical HDPE behavior. The exhumed sample exhibits fragile behavior for one of the test specimens tested, without deformation prior to rupture. The Geosynthetic Research Institute criteria require a minimum of 700% in the tensile break elongation and the average value of the exhumed sample was 482.63% with a high standard deviation. Therefore, it was observed which exhumed sample had a change in the tensile behavior, probably caused by the weather conditions, as UV radiation and high temperatures. The tear test results did not show similar behaviors for both samples tested, despite the fact that the samples presented tear resistance in accordance with the Geosynthetic Research Institute criteria. Figs. 13 and 14 show the puncture test curves for the exhumed and reference samples, respectively. The puncture test curves showed different behaviors for both samples tested. The reference sample presented a typical HDPE curve. However, the exhumed sample presented a higher elongation at the break than the reference sample.

4. Conclusions

The exhumed high-density polyethylene geomembrane sample and the reference sample were evaluated by the TG, differential scanning calorimetry, TMA, and physical analyses to analyze the behavior of the sample after exposure to an industrial water pond for 2.25 years.

TG used at different heating rates under synthetic air purge gas evaluation showed that the exhumed sample presented a different behavior in the TG curve for a heating rate of 5 °C due to the effect of the reaction time. The DTG behavior showed that the overlapping reactions tend to decrease gradually when the heating rate is increased for the exhumed sample. The reference sample showed the tendency to decrease the number of decomposition reactions with the increase in heating rates. The DTG curves under carbonic purge gas indicate a homogeneous behavior of the thermal decomposition reaction, except for the heating rates of 5 °C, which presented a shoulder at the beginning of the thermal decomposition for both samples. The activation energy values showed that the samples have a different kinetic behavior in both purging gases used. For the reference and exhumed sample, and that in synthetic air, the activation energy values were the same while for the carbon dioxide purge gas, there were differences in the initial thermal decomposition values.

The DTA curves showed the endothermic peaks between 120 and 140 °C and different DTA curve behaviors since the second stage of decomposition between the samples. The DSC curves showed similar glass transition and melting peaks for both samples. For the analysis of 10 °C min^{-1} in the melting point, the exhumed sample has an overlapping reaction while the reference sample did not have an overlapping reaction.

The TMA curves without purge gas showed the range of thermal stability between 30 and 65 °C for the reference sample, which is

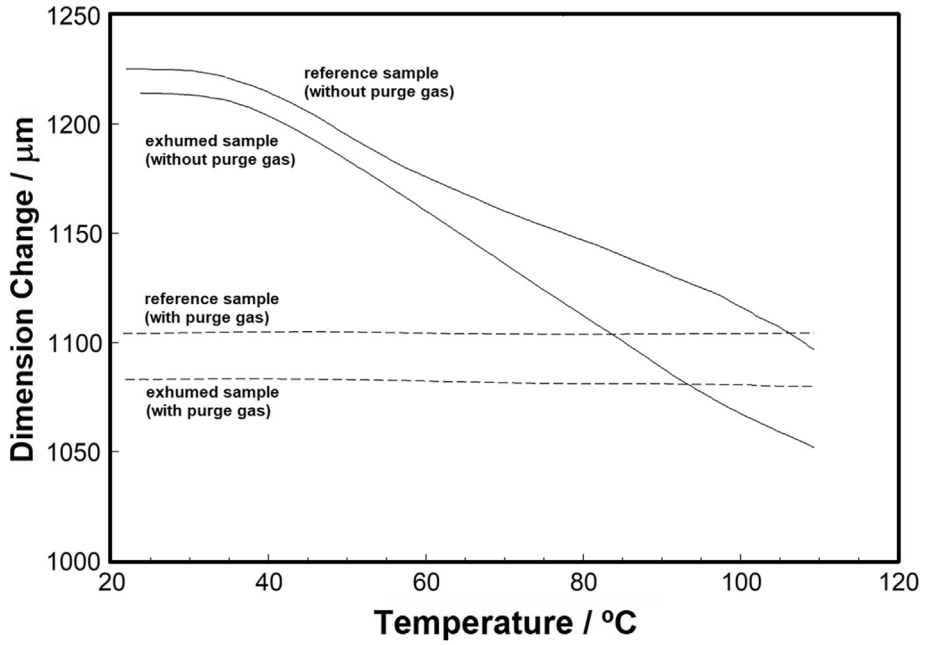

Fig. 10. TMA curves for heating rate of 5 °C min^{-1} under nitrogen purge gas.

Table 4
Physical properties of the high-density polyethylene geomembrane samples evaluated.

Samples	Thickness/(mm)	Density/(g/cm^3)	MFR/(g/10 min)
GM 1L Virgin	1.040 (±0.079)	0.958 (±0.002)	0.6800 (±0.0217)
GM CLIQ Exhumed	0.998 (±0.095)	0.943 (±0.002)	0.4256 (±0.0079)

The standard deviations are shown between brackets.

attributed to molecular relaxation. The exhumed sample did not have the same relaxation, probably because this sample was submitted to severe environmental conditions in the field.

The physical property values showed typical HDPE values for the reference sample. Besides, for the exhumed sample, the physical properties values showed lower melt flow rates, different puncture curve behavior and tensile brittle behavior which can indicate that changes probably occurred in the polymer structure for the exposed sample.

The analyses made in this paper showed important similarities between the samples studied. The TG analysis demonstrates similar behaviors in the curves at heating rates of 10, 20 and 30 ºC. For the DTG

Table 5
Physical properties of the high-density polyethylene geomembrane samples evaluated.

Samples	Tens. yield resist./(kN m^{-1})	Tens. yield elong./ (%)	Tens. break resist./(kN m^{-1})	Tens. break elong./ (%)	Tear resist./ (N)	Puncture resist./ (N)	Puncture elong./ (mm)
GM 1L Virgin	21.07 (±1.66)	12.61 (±2.48)	28.52 (±1.55)	733.47 (±10.76)	169.17 (±8.76)	434.17 (±18.19)	12.93 (±0.10)
GM CLIQ Exhumed	18.57 (±0.20)	14.61 (±1.47)	21.98 (±6.82)	482.63 (±329.65)	145.50 (±3.29)	473.23 (±35.22)	22.67 (±4.92)

The standard deviations are shown between brackets.

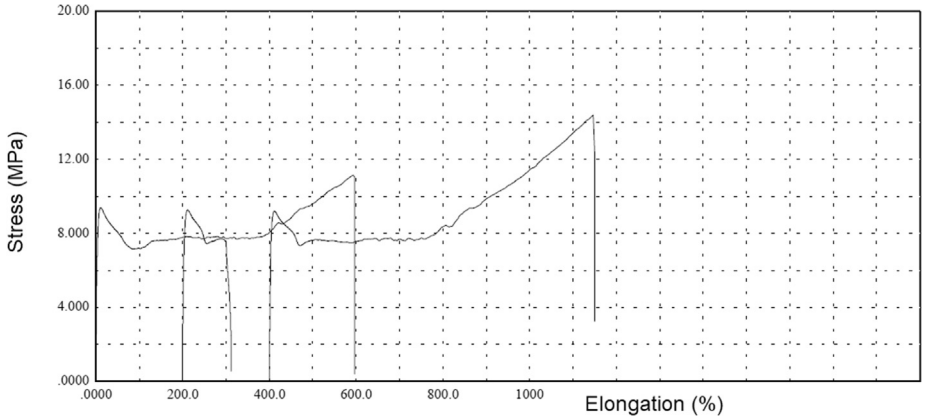

Fig. 11. Tensile test curves for the exhumed sample.

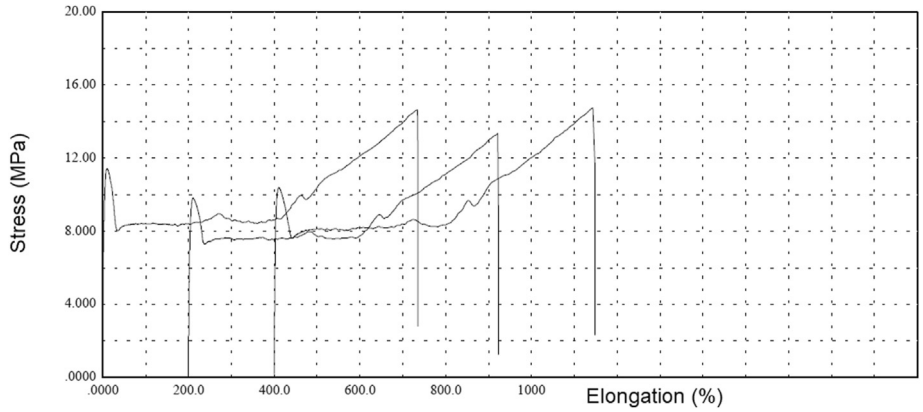

Fig. 12. Tensile test curves for the reference sample.

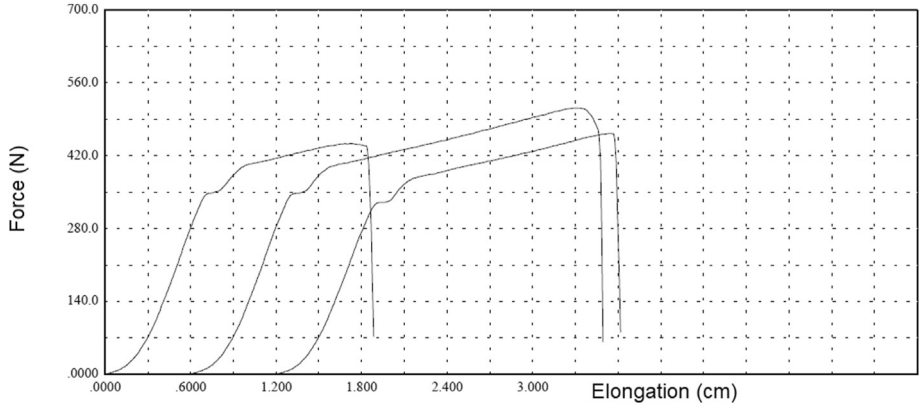

Fig. 13. Puncture test curves for the exhumed sample.

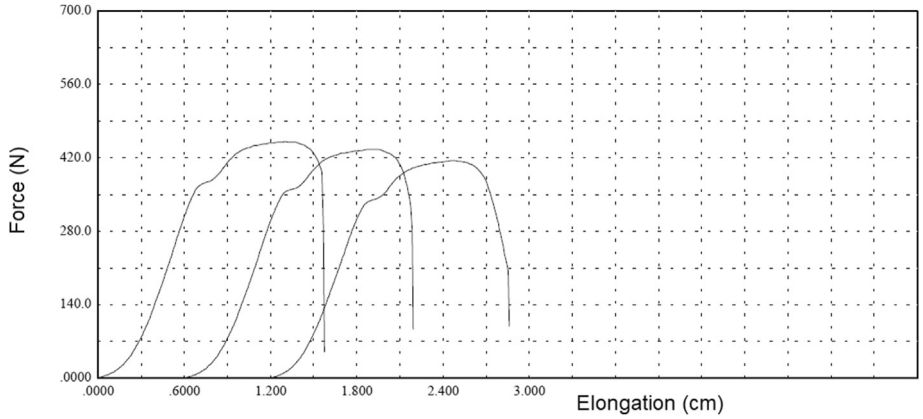

Fig. 14. Puncture test curves for the reference sample.

analysis, the reference sample presented a synthetic air thermal decomposition similar to that observed for Valentin et al. [20], who evaluated four different Brazilian virgin HDPE geomembranes. Under carbonic purge gas, the DTG samples curves for the heating rates of 10, 20 and 30 ºC indicate a homogeneous behavior of the thermal decomposition reaction. The DTA curves showed similarities between the samples in the endothermic peak. As can be seen in the DSC curves, the melting points and the glass transition between the samples presented similar behaviors. For the TMA analysis, both samples, without purge gas, obtained the thermal stability until a temperature of about 30 ºC. For the analysis without a purge gas condition, both samples present the same and distinct behavior, with no changes in the thickness.

In conclusion, the similarities between the samples studied demonstrated the same polymer behavior, and the differences between the samples verified in those analyses can indicate that changes probably occurred in the polymer structure for the exposed sample. The changes noted in the exhumed sample highlight the importance of an additive package to efficiently protect the polymer during its lifetime, which can

be degraded by UV radiation, thermal and oxidative mechanisms.

Credit author statement

Fernando Luiz Lavoie: Conceptualization (lead); Investigation (lead); Project administration (supporting); Resources (lead); Supervision (lead); Validation (supporting); Visualization (lead); Writing - original draft Preparation (lead); Writing - review & editing (lead). Marcelo Kobelnik: Conceptualization (supporting); Formal analysis (lead); Investigation (supporting); Validation (lead); Visualization (supporting); Writing - original draft Preparation (supporting); Writing - review & editing (supporting). Clever Aparecido Valentin: Formal analysis (supporting); Investigation (supporting); Resources (supporting); Validation (supporting); Visualization (supporting); Writing - original draft (supporting). Jefferson Lins da Silva: Conceptualization (supporting); Project administration (lead); Writing - review & editing (supporting). Maria de Lurdes Lopes: Conceptualization (supporting); Writing - review & editing (supporting).

Data availability

The raw/processed data required to reproduce these findings cannot be shared at this time due to technical or time limitations.

Declaration of competing interest

The authors declare that they have no known competing financial interests or personal relationships that could have appeared to influence the work reported in this paper.

References

[1] A.R. Rollin, J.M. Rigo, Geomembranes: Identification and Performance Testing, Chapman and Hall, 1991.

[2] R.M. Koerner, Designing with Geosynthetics, Prentice Hall Publ. Co., Englewood Cliffs, 2005. New Jersey.

[3] J.C. Vertematti, Brazilian Handbook of Geosynthetics, Blücher, São Paulo, 2015 (in Portuguese).

[4] E.M. Palmeira, Geosynthetics in Geotechnics and Environment, Oficina de Textos, São Paulo, 2018 (in portuguese).

[5] R.K. Rowe, H.P. Sangam, Durability of HDPE geomembranes, Geotext. Geomembranes 20 (2002) 77–95, https://doi.org/10.1016/S0266-1144(02)00005-5.

[6] A.K. Sahu, K. Sudhakar, R.M. Sarviya, Influence of U. V light in thermal properties of HDPE/Carbon black composites, Case Studies in Thermal Engineering 15 (2019) 100534, https://doi.org/10.1016/j.csite.2019.100534.

[7] G. Davis, The characterization of two different degradable polyethylene (PE) sacks, Mater. Char. 57 (2006) 314–320, https://doi.org/10.1016/j.matchar.2006.02.014.

[8] D. Kay, E. Blond, J. Mlynarek, Geosynthetics durability: a polymer chemistry issue, in: 57th Canadian Geotechnical Conference, Québec, Canada', 2004.

[9] K. Majewski, S.C. Mantell, M. Batthacharya, Relationship between morphological changes and mechanical properties in HDPE films exposed to a chlorinated environment, Polym. Degrad. Stabil. 171 (2020) 109027, https://doi.org/10.1016/j.polymdegradstab.2019.109027.

[10] G.R. Koerner, Y.G. Hsuan, R.M. Koerner, The durability of geosynthetics, in: R.W. Sarsby (Ed.), Geosynthetics in Civil Engineering, Woodhead Published Limited, Cambridge, 2007, pp. 36–65.

[11] L.C. Mendes, E.S. Rufino, F.O.C. de Paula, A.C. Torres Jr., Mechanical, thermal and microstructure evaluation of HDPE after weathering in Rio de Janeiro City, Polym. Degrad. Stabil. 79 (2003) 371–383, https://doi.org/10.1016/S0141-3910(02)00337-3.

[12] Y.G. Hsuan, R.M. Koerner, The single point-notched constant tension load test: a quality control test for assessing stress crack resistance, Geosynth. Int. 2 (1995) 831–843, https://doi.org/10.1680/gein.2.0038.

[13] Y.G. Hsuan, R.M. Koerner, Antioxidant depletion lifetime in high density polyethylene geomembranes, J. Geotech. Geoenviron. Eng. 124 (1998) 532–541, https://doi.org/10.1061/(ASCE)1090-0241(1998)124:6(532).

[14] A.M. Noval, M. Blanco, F. Castillo, A. Leiro, B. Mateo, J.G. Zornberg, E. Aguiar, J.B. Torregrosa, M. Redón, Long-term performance of the HDPE geomembrane at the "San Isidro" reservoir, in: 10th International Conference on Geosynthetics, 2014. Berlin, Germany.

[15] D.H. Mitchell, Geomembrane compatibility tests using uranium acid leachate, Geotext. Geomembranes 2 (1985) 111–127, https://doi.org/10.1016/0266-1144(85)90002-0.

[16] J.S. Dix, J.R. Burkinshaw, HDPE resin developments, Geotext. Geomembranes 10 (1991) 621–624, https://doi.org/10.1016/0266-1144(91)90052-X.

[17] P.C. Lodi, B.S. Bueno, Thermo-gravimetric analysis (TGA) after different exposures of high density polyethylene (HDPE) and polyvinyl chloride (PVC) geomembranes, Electron. J. Geotech. Eng. 17 (2012) 3339–3349.

[18] F.L. Lavoie, B.S. Bueno, P.C. Lodi, Waterproofing membrane degradation of high-density polyethylene used in storage vinasse tanks, Polímeros 23 (5) (2013) 690–695, https://doi.org/10.4322/polimeros.2013.010 (in portuguese).

[19] F.B. Abdelaal, R.K. Rowe, Y.G. Hsuan, R. Awad, Effect of high temperatures on the physical and mechanical properties of HDPE geomembranes in air, Geosynth. Int. 22 (2015) 207–223, https://doi.org/10.1680/gein.15.00006.

[20] C.A. Valentin, J.L. Silva, M. Kobelnik, C.A. Ribeiro, Thermoanalytical and dynamic mechanical analysis of commercial geomembranes used for fluid retention of leaching in sanitary landfills, J. Therm. Anal. Calorim. (2018), https://doi.org/10.1007/s10973-018-7690-0.

[21] ASTM D 5199, Standard Test Methods for Measuring the Nominal Thickness of Geosynthetics, 2012.

[22] ASTM D 792, Standard Test Methods for Density and Specific Gravity (Relative Density) of Plastics by Displacement, 2013.

[23] ASTM D 1238, Standard Test Methods for Melt Flow Rates of Thermoplastics by Extrusion Plastometer, 2013.

[24] ASTM D 6693, Standard Test Methods for Determining Tensile Properties of Nonreinforced Polyethylene and Nonreinforced Flexible Polypropylene Geomembranes, 2015.

[25] ASTM D 1004, Standard Test Methods for Tear Resistance (Graves Tear) of Plastic Film and Sheeting, 2013.

[26] ASTM D 4833, Standard Test Methods for Index Puncture Resistance of Geotextiles, Geomembranes, and Related Products, 2007.

[27] M. Fonseca, L.M.B. Ferreira, R.A.M. Soares, M. Kobelnik, G.G. Fontanari, M.S. Crespi, C.A. Ribeiro, Extraction of soursop oil (Annona muricata L.) by ultrasonic technique Chromatographic evaluation and thermal characterization, J. Therm. Anal. Calorim. 134 (2018) 1893–1901, https://doi.org/10.1007/s10973-018-7753-2.

[28] M. Kobelnik, G.G. Fontanari, R. Soares, Study of the thermal behavior of bicuiba oil (Virola bicuyba), J. Therm. Anal. Calorim. 115 (2014) 2107–2113, https://doi.org/10.1007/s10973-013-3315-9.

[29] GRI—GM13, Test Methods, Test Properties and Testing Frequency for High Density Polyethylene (HDPE) Smooth and Textured Geomembranes SM, Geosynthetic Institute, 2019.